IEEE Access
Multidisciplinary | Rapid Review | Open Access Journal

Received 28 August 2023, accepted 15 October 2023, date of publication 18 October 2023, date of current version 27 October 2023.

Digital Object Identifier 10.1109/ACCESS.2023.3325632

RESEARCH ARTICLE

Evaluation of Sustainable Design Method for Three-Lane Entrance Ramps on Expressways in Urban Areas: A Case Study of Xi'an, China

YUTONG LIU[1], BINGHONG PAN[1], RUIHUA SONG[1], AND LIN ZONG[2]
[1]Highway Academy, Chang'an University, Xi'an 710064, China
[2]Shanghai Fengxian District Construction and Transportation Commission, Shanghai 201499, China

Corresponding author: Binghong Pan (Panbh@chd.edu.cn)

This work was supported in part by the Scientific Research Program funded by the Shaanxi Provincial Education Department, under Grant 21JK0908.

ABSTRACT Owing to the challenges faced by two-lane entrance ramps in merging areas on expressways in handling the growing traffic volume, designers are considering implementing three-lane entrance ramps. This approach alleviates capacity bottlenecks and facilitates efficient, safe, and green operations. However, according to the traditional design strategy, the long auxiliary lanes will bring large land occupation and construction consumption, creating obstacles to the reconstruction. To address this issue, this study proposes two new strategies and discusses the applicability of each scheme. A VISSIM microsimulation model was developed and calibrated using the collected data, and five evaluation indicators assessing environmental protection, capacity, traffic efficiency, safety, and construction consumption were selected. This study also presents a comprehensive evaluation(CE) method that combines the CRITIC (Criteria Importance Through Intercriteria Correlation) method and TOPSIS(Technique for Order Preference by Similarity to an Ideal Solution), which considers the association between indicators and offers a more rational evaluation, aiming to recommend optimal designs for various traffic cases. The results indicate that two-lane ramps are still the preferred choice for lower traffic volumes and merging ratios, whereas three-lane ramps demonstrate excellent potential for application under heavy traffic conditions. The CE reveals substantial improvements in optimal designs, with capacity, delay, CO emissions, and conflicts showing maximum enhancements of approximately 20%, 45%, 5%, and 55%, respectively.

INDEX TERMS Expressway, three-lane entrance ramp, design method, CE, sustainable transportation, low carbon.

I. INTRODUCTION

Urban expressways function as main transportation arteries, taking the essential task of efficient transportation. However, with the increasing population density and motor vehicle ownership in cities, there are pressing needs for urban road reconstruction and expansion to fulfill residents' escalating transportation demands.

Exits and entrances on urban expressways, which play a vital role in traffic flow transitions, emerge as decisive factors affecting the overall operating quality of expressways and have been generally regarded as the bottleneck section. Frequent lane changes in merging areas invariably result in more complicated traffic conditions, even causing disruptions in the traffic flow on the mainline. As a result, merging areas frequently experience heightened congestion and conflicts compared to general sections [1], [2], [3]. Studies have also provided statistical data to indicate significantly higher crash rates in the merging area [4], [5], [6].

Additionally, issues about rising fuel consumption and pollutant emissions from congestion and conflicts have drawn considerable attention [7], [8]. Notably, despite that emission standards are constantly being improved, extreme congestion can offset the benefit and further exacerbate the pollution problem [9]. Research indicates that emissions significantly increase during the transition of traffic flow from free to

The associate editor coordinating the review of this manuscript and approving it for publication was Daniela Cristina Momete.

congestion [10]. Emissions produced by motor vehicles in urban settings have recently drawn special attention due to the increasing emphasis on sustainability [11], [12].

Cities have achieved certain progress in congestion and emission management by formulating and implementing restriction policies [13], [14], [15]. However, these tactics obstruct urban development and even conflict with rising living and production standards. Furthermore, studies have concluded that these restriction strategies provide limited benefits and may foster new contradictions over the long term, triggering a backlash in congestion and emissions [16], [17], [18].

Based on observations and data collection of traffic flow, several prediction models have been developed to analyze the characteristics of traffic flow in the merging areas. These models offer valuable approaches for reducing congestion and emissions by predicting speed variations, capacity, and driver's behavior [19], [20], [21], [22]. Furthermore, researchers work on devising innovative traffic strategies, including coordinated control of speed and lanes as well as presenting new path designs [23], [24], [25]. While integrating road pricing with other strategies helps alleviate traffic pressure at interchanges to some extent, these approaches may inevitably have negative effects on drivers and passengers [26], [27].

Discussions also focused on the theme of planning and design of expressway entrances. Based on observations and documentation of ramps, scholars have evaluated the effects of geometric design and traffic volume on congestion, safety, and other multifaceted operational benefits [28], [29]. Studies about multi-lane entrance ramps highlight advantages associated with additional auxiliary lanes [30], [31]. However, the omission or shortening of auxiliary lanes does not appear to significantly affect operational efficiency in certain conditions [32]. The detrimental impact of overflow traffic from ramps on the capacity in merging areas has also been established, suggesting a correlation between the number of lanes and capacity bottlenecks [33], [34]. These studies provide important references and inspiration for the design of three-lane ramps. With mainline lanes expanding from the initial two to four or even five, there has been a substantial increase in capacity. Accordingly, it can be hypothesized that augmenting the number of ramp lanes can effectively mitigate on-ramp queue lengths and prevent spillbacks by enhancing storage capacity, which will break the capacity bottleneck in the merging areas.

Actual observations may not be available for some new traffic strategies or design schemes since they have not been constructed. Perhaps their digital twin would be a better object for the study. In recent years, numerical simulation techniques such as the VISSIM have been introduced and widely utilized for transportation, and have been proven the effectiveness and reliability [35], [36]. For accurate and reliable results, the simulation model must realistically represent the characteristics of the actual traffic flow and microscopic driving behavior. Consequently, studies propose and optimize the VISSIM modeling and calibration procedure [37], [38], [39]. By accurately developing and calibrating the simulation model, it is possible to closely restore traffic flow in the merging areas, thereby providing a solid foundation for evaluation [40].

Multi-criteria decision-making (MCDM) is based on the principles of operations research, assigning weights to selected indicators in scheme evaluation. In this way, it provides scoring details for schemes decision-making in complex cases [41]. Among that, the commonly used methods include the entropy method and the CRITIC method. The entropy method calculates weights based on the variability degree of indicators using information entropy, having shown promising results in evaluating sustainable transportation designs [42], [43]. However, the entropy method has inherent limitations because it fails to account for the correlation between indicators. In contrast, the CRITIC method effectively addresses this problem by introducing contrast intensity and correlation indicators [44]. Currently, the CRITIC method has gained widespread applications not only in transportation [45], [46], [47] but also in diverse fields such as manufacturing [48], construction [49], medicine [50], energy, and environment [51].

Furthermore, as another significant MCDM method, the TOPSIS has also been widely used in various disciplines [52], [53], [54]. The TOPSIS is an intragroup comprehensive evaluation method that effectively utilizes information from the original data and provides an accurate reflection of gaps between schemes [55].

Currently, expressway entrance ramps typically consist of one or two lanes, which is inadequate to meet escalating transportation demands in certain cases. The implementation of three-lane ramps may be a key solution to alleviate capacity bottlenecks in merging areas. However, current specifications lack specific guidance for the three-lane design. Consequently, the primary challenge for designers is determining an appropriate design strategy, particularly regarding merging path planning and geometric design in the merging areas. Following the conventional design strategy, the connection and transition between a three-lane ramp and the mainline should be established by two auxiliary lanes. However, this requirement will result in increased land and resource consumption in construction, while the expansion of urban expressways is often hampered by limited land resources.

This study aims to propose a sustainable three-lane entrance design method with the applicability evaluation of the design using MCDM. Inspired by a special two-lane entrance ramp without an auxiliary lane on the Xi'an Ring Expressway, three design schemes for three-lane entrances with different traffic organization methods and geometric forms were proposed. To assess the quantified performance of each design in terms of environmental protection, efficiency, and safety under various traffic scenarios, a VISSIM model

is developed and calibrated based on measured traffic data. Finally, CE combining the CRITIC method and TOPSIS scores each design and suggests the optimal design for different traffic scenarios.

The remainder of this paper is organized as follows. Section II introduces the research methodology, including data collection, scheme design, numerical simulation, and evaluation. Section III provides an overview of data collection and scheme design. The simulation and evaluation results, along with the sensitivity analysis, are presented in Section IV. Section V discusses the findings of the study, and conclusions are presented in Section VI.

II. METHODOLOGY

A. FIELD DATA COLLECTION

Accurate traffic data are essential for supporting the analysis and evaluation. Data collection should be scheduled during rush hour, but without accidents, obvious congestion, and facility maintenance to minimize disturbances to drivers. These details should be determined based on prior investigations [56]. The following data should be collected.

- Traffic volume on the mainline and the ramp approaching the merging nose.
- Vehicle speeds on the mainline and the ramp approaching the merging nose.
- Proportion of trucks and buses within the traffic flow.

B. IMPROVEMENT SCHEME DESIGN

This study focuses on the development of sustainable designs for three-lane entrance ramps, including traffic characterization and applicability evaluation. Currently, the specification has not proposed the design method for three-lane ramps. Following the conventional design strategy for two-lane ramps, lengthy auxiliary lanes are required in the three-lane ramp design scheme, resulting in substantial land and resource consumption in the construction. Therefore, this study proposes various schemes with different auxiliary lane designs for three-lane ramps, matching specific traffic characteristics.

C. DEVELOPMENT AND CALIBRATION OF SIMULATION MODEL

1) MODEL DEVELOPMENT

Because almost no three-lane ramps have been constructed yet, it is difficult to observe and analyze their operational performance directly. Therefore, the evaluation uses the VISSIM micro-simulation to replicate both existing and optimized schemes. Each detail is set closely to resemble the actual conditions, including geometric parameters, traffic characteristics, and vehicle paths.

2) MODEL CALIBRATION

To enhance the fidelity of the VISSIM simulation model, calibration is necessary to align it more closely with actual conditions. Calibration parameters typically include gap acceptance, car-following, and lane-changing models [57]. Previous studies have employed capacity as a calibration indicator because it directly reflects the accuracy of the VISSIM model. The mean absolute percentage error (MAPE) is commonly utilized as an evaluation indicator to quantify the error between the VISSIM model and reality. (1) shows the MAPE calculation process [42], [43].

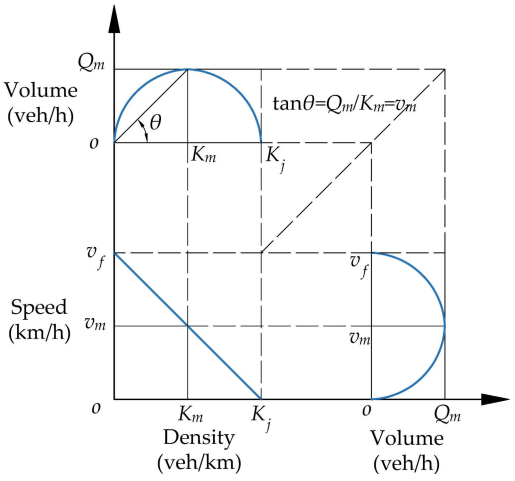

FIGURE 1. Relationships between the three traffic paraments. K_j denotes the jam density, v_m denotes the critical speed, Q_m denotes the maximum volume, K_m denotes the optimal density which takes half of K_j, and v_f denotes the smooth speed as density approaches 0.

$$MAPE_C = \frac{\sum_{i=1}^{n} C_v^i + \sum_{i=1}^{n} C_f^i}{\sum_{i=1}^{n} C_f^i} \tag{1}$$

where C_v^i denotes the simulated capacity in the VISSIM model (veh/h), while C_f^i denotes the investigated capacity, i denotes the traffic flow, and n denotes the total through and merging traffic flows.

Given that relying on a single indicator may not be sufficient for calibration purposes, vehicle density, which is another of the three traffic parameters, is also considered, as shown in (2). Furthermore, the speed precision can be inferred from the precision of capacity and vehicle density based on the relationship between the three traffic parameters.

$$MAPE_K = \frac{\sum_{i=1}^{n} K_v^i + \sum_{i=1}^{n} K_f^i}{\sum_{i=1}^{n} K_f^i} \tag{2}$$

where K_v^i denotes the simulated vehicle density in VISSIM (veh/km), K_f^i denotes the investigated vehicle density.

In addition, it is necessary to calibrate the simulation for more traffic conditions because of the dynamic nature of traffic. Following the Greenshields Model, both volume and density initially increase concurrently in real traffic flow. The maximum volume occurs when the density reaches half the jam value. Similarly, the interrelationship between the three traffic parameters can be deduced, as shown in Figure 1.

Results obtained from the VISSIM simulation for the three traffic parameters can be used for the fit of a quadratic

polynomial to K and Q. Additionally, the goodness of fit, as measured by the coefficient of determination, enables the assessment of the compatibility between the Greenshields Formula and the observed data.

3) INDEXES SELECTION

The operational performance evaluation of each design scheme should encompass considerations of the environmental impact, transportation efficiency, and safety. Commonly employed nodes results in VISSIM analysis, including CO and NOx emissions, fuel consumption, travel time, delay, and the number of stops [58], [59]. In addition, the Federal Highway Administration introduced the Surrogate Safety Assessment Model, predicting and evaluating traffic conflicts from trajectory data generated by VISSIM. This model has been extensively employed and validated [60].

For three-lane ramps, the primary improvement effect should be reflected in capacity, which can be quantified by the number of vehicles in the VISSIM results. Additionally, this study also considers representative CO emissions, delays, and the number of conflicts as other indicators for evaluating sustainability. The merging areas have distinctive lengths in each design, owning to the variance in the auxiliary lane configurations. Because partial indicators are directly related to the travel distance of vehicles, it is crucial to control this variable during the simulation. Hence, this study opts for the selection of the same range of nodes for simulation data collection, which should cover the longest merging area.

D. SENSITIVITY ANALYSIS OF SCHEME PERFORMANCE

Due to the dynamic nature of traffic operations, further research is required to examine the applicability of these designs in additional traffic scenarios beyond the investigation. Considering that the traffic volume and diverging ratio play crucial roles in controlling the formation of capacity bottlenecks, they can be selected as control variables. A sensitivity analysis is necessary to explore how the indicators vary with these variables.

E. COMPREHENSIVE EVALUATION METHODOLOGY

1) EVALUATION METHOD

Sustainable transportation encompasses not only the enhancement of transportation efficiency but also the mitigation of environmental impact. In particular, the environmental impact is not limited to the reduction in fuel consumption and pollutant emissions during operation, and the burden of construction also cannot be ignored. Schemes with larger construction volumes lead to increased consumption of materials and resources. Moreover, they encroach upon more land resources and jeopardize existing ecology. Achieving sustainability goals requires a balance between these aspects.

Therefore, it is necessary to adopt the CE method to allocate weights to individual indicators, thereby scoring each design scheme. Specific indicators to support the evaluation should include capacity, delay, CO emissions, the number of conflicts, and construction costs. Several factors, such as resource consumption, construction time, and labor input, are involved in construction, but not all of them can be quantitatively expressed because of their variability based on project conditions. Therefore, the additional area is selected as the fifth indicator, which is consistent with all other cost considerations. The additional square can be defined as the additional area of the new scheme over the original scheme within the mainline, including the auxiliary lanes and taper.

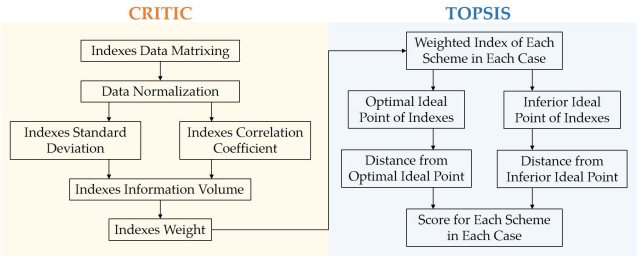

FIGURE 2. Flowchart of the CE method.

Since evaluation indicators originate from different fields and exhibit different quantitative levels, an intuitive approach is insufficient. Therefore, this study proposes the utilization of the CE method that incorporates the CRITIC and TOPSIS methods to score the performance of each scheme, providing comprehensive support for the decision-making processes.

The TOPSIS ranks evaluation objects by their proximity to idealized targets. It avoids subjectivity and portrays the comprehensive impact intensity of various indicators without strict limitations on sample volume, and has been widely utilized in objective scheme scoring. However, before applying the TOPSIS, the entropy method is usually employed for weight assignment. Although the entropy method provides a brief objective weighting process, some defects cannot be ignored, as they fail to consider the effects between indicators. As a complex and integrated system, road traffic data inherently contain connections and fluctuations, which matches the feature of the CRITIC method. Figure 2 illustrates the CE method process.

2) WEIGHT ASSIGNMENT BASED ON CRITIC METHOD

Objective weight assignment methods, such as entropy and standard deviation methods, primarily focus on the data itself. They overlook the volatility and correlation among the data, which hold valuable information. In contrast, the CRITIC method effectively capitalizes on these characteristics by employing two key indices: the volatility (contrast intensity) and the conflict (correlation). The contrast intensity, represented as the standard deviation, assigns higher weights to indices exhibiting greater fluctuations. The conflict can be quantified by the correlation coefficient, where the higher coefficient indicates the lower conflict and weight conversely. Following the normalization, each weight was calculated by multiplying the contrast intensity by the conflict of the index. Through this approach, the evaluation will be

not solely reliant on the magnitude of each index, but also incorporates the objective nature of the data, thereby facilitating a scientific and comprehensive evaluation.

In each case, each design is evaluated with five indicators, and the matrix A_k for the original data in the k^{th} case can be constructed, as shown in (3).

$$A_k = \begin{bmatrix} V_{1,k} & D_{1,k} & E_{1,k} & C_{1,k} & S_{1,k} \\ V_{2,k} & D_{2,k} & E_{2,k} & C_{2,k} & S_{2,k} \\ \cdots & \cdots & \cdots & \cdots & \cdots \\ V_{i,k} & D_{i,k} & E_{i,k} & C_{i,k} & S_{i,k} \end{bmatrix} \tag{3}$$

where $V_{i,k}$ denotes the number of vehicles of i^{th} design in k^{th} case, and $D_{i,k}, E_{i,k}, C_{i,k}, S_{i,k}$ denote the delay, CO emissions, number of conflicts, and additional square, respectively.

Due to the different measurement units for each indicator, it is necessary to normalize each set of data to solve the problem of homogenization of different qualitative indicators. Considering that all five indicators are expected to exhibit lower numerical values, each of them is essential to be reverse-processed. Initially, elements in A_k are denoted as x_{ij}, where i represents the i^{th} design and j represents the j^{th} index in the order of V, D, E, C and S. Then A_k should be transformed into X as described in (4).

$$X = \begin{bmatrix} x_1 & x_2 & x_3 & x_4 & x_5 \end{bmatrix} \tag{4}$$

where x_j can be denoted as (5).

$$X = \begin{bmatrix} x_{1j} & x_{2j} & \cdots & x_{ij} \end{bmatrix}^T \tag{5}$$

The inverse normalization for x_{ij} can be processed from (6).

$$x'_{ij} = \frac{max\{x_{1j}, x_{2j}, \ldots, x_{ij}\} - x_{ij}}{max\{x_{1j}, x_{2j}, \ldots, x_{ij}\} - min\{x_{1j}, x_{2j}, \ldots, x_{ij}\}} \tag{6}$$

As one of the key indices of the CRITIC method, the contrast intensity is expressed as the standard deviation, calculated as in (7) and (8).

$$\overline{x'_j} = \frac{1}{n\sum_{i=1}^{n} x'_{ij}} \tag{7}$$

$$S_j = \sqrt{\frac{\sum_{i=1}^{n}(x'_{ij} - \overline{x'_j})^2}{n-1}} \tag{8}$$

where S_j denotes the standard deviation of the j^{th} indicator and n denotes the number of design schemes.

The standard deviation is a measure of the fluctuation in the values of each indicator. A higher standard deviation indicates a greater variation in the indicator values, providing more information and stronger evaluation intensity, thereby a higher weight should be assigned to these indicators. As another crucial factor, the conflict between indicators is expressed using the correlation coefficient, as shown in (9).

$$R_j = \sum_{j'=1}^{m}(1 - r_{j,j'}) \tag{9}$$

where $r_{j,j'}$ denotes the correlation coefficient of the j^{th} and j'^{th} indicators, m denotes the number of indicators.

Within the CRITIC method, the stronger correlation between two indicators indicates less conflict, which shows the same information and repeated details in the evaluation. Consequently, the evaluation intensity of that indicator should be weakened, and the weight assigned to it should be reduced. The information volume is calculated using (10).

$$C_j = S_j \times \sum_{j'=1}^{m}(1 - r_{j,j'}) = S_j \times R_j \tag{10}$$

As C_j increases, the j^{th} indicator plays a more significant role. Therefore, more weight should be assigned to it, whereas the objective weight of the j^{th} index in the k^{th} case can be calculated using (11).

$$w_{k,j} = \frac{C_j}{\sum_{j=1}^{m} C_j} \tag{11}$$

3) EVALUATION BASED ON THE TOPSIS

The TOPSIS is a frequently used intragroup evaluation method, that effectively utilizes information from the original data and provides an accurate reflection of the gaps between schemes. Utilizing a normalized original data matrix, the TOPSIS employs the cosine method to determine the optimal and worst schemes from available options. Subsequently, it calculates the distance between each evaluation object with the optimal and worst schemes to establish their proximity, serving as evidence for evaluation. Given that the weights for each indicator in each case have already been calculated using the CRITIC method, the TOPSIS model can be conveniently employed for the final scoring. The steps outlined are as follows:

The weighted index of the i^{th} design in the k^{th} case can be calculated using (12).

$$Z_{k,ij} = w_{k,j} \times x'_{ij} \tag{12}$$

The optimal and inferior ideal points of the j^{th} index are defined as the maximum and minimum weighted values of the five designs, respectively, as shown in (13) and (14).

$$Z_j^+ = max(Z_{ij}) \tag{13}$$

$$Z_j^- = min(Z_{ij}) \tag{14}$$

The distances from the optimal and inferior ideal points to each indicator in the i^{th} case are defined by (15) and (16), respectively.

$$D_i^+ = \sqrt{\sum_{j=1}^{4}(Z_j^+ - Z_{ij})^2} \tag{15}$$

$$D_i^- = \sqrt{\sum_{j=1}^{4}(Z_j^- - Z_{ij})^2} \tag{16}$$

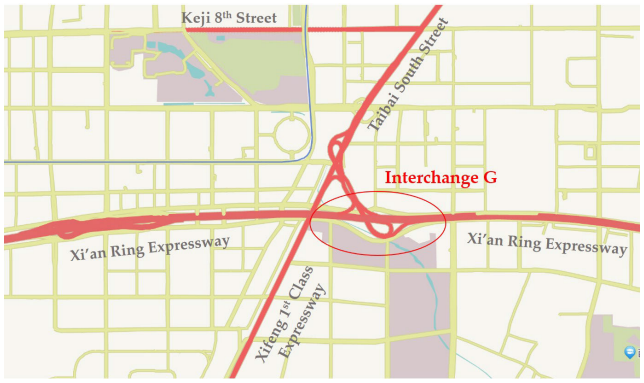

FIGURE 3. The location and type of Interchange *G*, which is a Trumpet-A type situated on the Xi'an Ring Expressway. The authors used the UAV to take aerial photos of the actual situation.

The score for the i^{th} design in the k^{th} case can be calculated using (17).

$$S_{k,i} = \frac{D_i^-}{D_i^+ + D_i^-} \tag{17}$$

III. DESCRIPTION OF DATA AND DESIGN

A. CASE DESCRIPTION

Figure 3 illustrates Interchange *G*, which is a Trumpet-A interchange situated on the Xi'an Ring Expressway. This interchange features a distinctive traffic organization in the merging area, where a two-lane entrance ramp directly connects to the mainline without an auxiliary lane. The main line of the expressway consists of six lanes at the speed limit of 120 km/h, and the ramp is operated at the speed limit of 60 km/h.

Expressways in urban areas typically exhibit the 24-hour traffic volume cycle, as well as heavy congestion occurs during peak hours. Xi'an, where Interchange *G* is located, has a resident population of over 13 million, with a density of 7.1 thousand people per square kilometer in the major urban area, and the number of motor vehicles in Xi'an has reached 3.736 million. Despite the introduction of a traffic restriction policy in Xi'an in 2019, it is hardly the fundamental strategy under the trend of continuous traffic growth.

Currently, traffic volume on the Xi'an Ring Expressway is consistently close to saturation levels, and some two-lane entrance ramps have been struggling to deal with traffic flow during rush hours. Hence, this study focused on the conversion of Interchange G into a three-lane entrance ramp as well as evaluating the benefits. Since conventional designs with lengthy auxiliary lanes can result in resource wastage in certain situations, it is imperative to optimize the design to address spatial and cost-related concerns.

B. DATA COLLECTION

Figure 4 shows the average congestion delay index on the Xi'an Ring Expressway near Interchange G for a specific week, using data queried from the open access platform of AMAP, Ltd. s

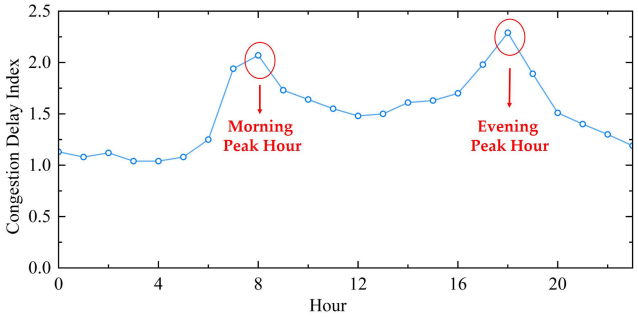

FIGURE 4. The average congestion delay index of the Xi'an Ring Expressway near Interchange *G* in a specific week. 8 denotes 8:00-8:59 a.m., and the other values indicate the same meaning.

TABLE 1. Trafffic data collection results of G interchange during rush hours.

Time	8:00-8:59 a.m.		5:00-5:59 p.m.	
Section	Mainline	Ramp	Mainline	Ramp
Car	2367	1572	2861	1790
Truck/Bus	314	61	326	56
Max. speed(km/h)	88.5	61.9	89.1	57.2
Min. speed(km/h)	34.3	44.7	27.9	24.8
Average speed(km/h)	63.4	51.8	59.7	39.3

FIGURE 5. The position of radars and the range for data collection. The red dot indicates the location of the radars, while the yellow square represents the range for data collection.

One-hour periods during the morning and evening rush hours are selected to conduct the research, being depicted in the data. Two radars were positioned approaching the merging nose on the mainline and ramp, as shown in Figure 5. The collected traffic data are presented in Table 1.

Traffic volume at the highest peak hour plays a decisive factor in road design, therefore the data from 5:00-5:59 p.m. were selected to be input into the VISSIM model. The following conclusions can be drawn from Table 1.

- The speed of vehicles on the mainline and the ramp was below the designed speed, at 59.7km/h and 39.3km/h respectively.
- Trucks and buses occurred in a low proportion less than 10%, and were restricted to the curb lane.

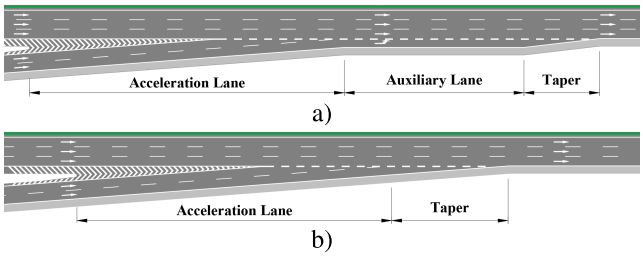

FIGURE 6. Two-lane entrance ramp designs. (a)CTE. (b)NTE.

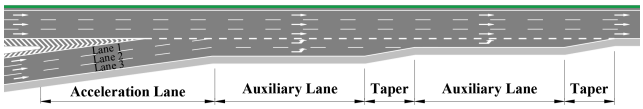

FIGURE 7. The double auxiliary-lane three-lane entrance(DATE) design.

- Merging vehicles accounted for nearly 40% of the total traffic.

Moreover, the UAV video shows that Chinese drivers always engage in aggressive driving behavior during congestion, such as occupying the emergency lane to merge into the mainline, which perhaps once again emphasizes the urgency of three-lane ramps.

C. DESIGN SCHEME

In the design of a two-lane entrance ramp, designers typically incorporate an auxiliary lane after the merging point to match the lane balance principle as recommended by AASHTO [61]. This design can be called the conventional two-lane entrance (CTE), which always provides better efficiency than the nonauxiliary-lane two-lane entrance(NTE), although it requires more space and expense. Figure 6 shows these two designs.

This study proposes three design schemes for three-lane entrance ramps based on CTE and NTE, with primary differences focusing on the auxiliary lane design. In the first scheme, the authors fully utilize the double-lane auxiliary lane in the merging area, which exclusively takes reference to the conventional strategy. This design can be called the double auxiliary-lane three-lane entrance(DATE), as shown in Figure 7. DATE strictly adheres to the lane balance principle, vehicles in the outermost lane on the ramp should merge into the mainline through two transitions, which can guarantee relatively smooth traffic under the heavy merging volume. However, this scheme requires over 1000m of auxiliary lane, significantly increasing construction costs and resource consumption.

To alleviate the construction pressure, a compromise design called the speed limit lane three-lane entrance (STE) is proposed. In this design, the first section of the two-lane auxiliary lane is shortened and transformed into a speed limit lane, as shown in Figure 8. Vehicles on the curb lane of the speed limit lane are subjected to a lower speed limit, providing more opportunities for lane changes to merge.

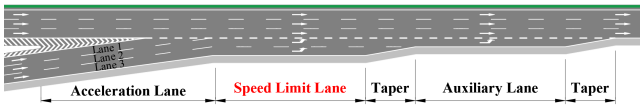

FIGURE 8. The speed limit-lane three-lane entrance(STE) design, replacing the first section of the auxiliary lane of DATE with a speed limit lane.

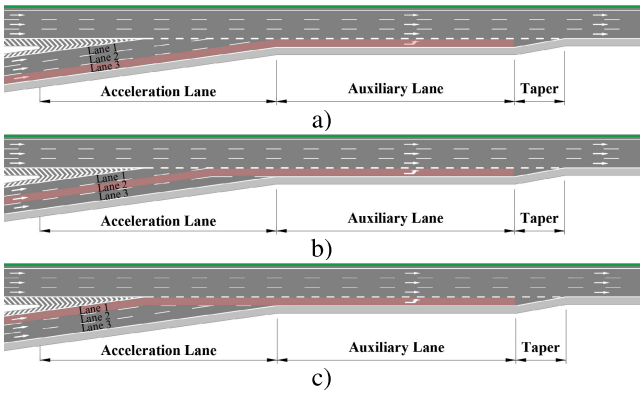

FIGURE 9. A single auxiliary-lane three-lane entrance (SATE) design. (a)Lane 3 on the ramp connects the auxiliary lane. (b)Lane 2 on the ramp connects the auxiliary lane. (c)Lane 1 on the ramp connects the auxiliary lane.

Traffic safety is the primary consideration on the speed-limited lane, therefore the length of the speed-limited lane should not be less than the stopping sight distance required for emergency braking. Although STE partially saves space and costs of construction, it poses the potential for reduced merging efficiency.

This study also proposes the single auxiliary-lane three-lane entrance(SATE) design, categorized into three distinct types as shown in Figure 9(a), (b), and (c), respectively. The difference between the three designs is reflected in the connecting targets of each lane of the ramp. In Figure 9(a), Lane 3 is connected to the auxiliary lane, while vehicles on Lanes 1&2 merge directly into the mainline, which may disrupt the traffic flow and present an accident hazard. Figure 9(c) shows the contrary, the auxiliary lane directly connected to Lane 1, traffic on Lanes 2&3 must merge into the mainline through the auxiliary lane. The design in Figure 9(c) may have the least impact on the mainline among the three designs, and might be optimal from the subjective view. However, it is still necessary to provide certain objective results to support the judgment.

As almost no three-lane ramps have yet been constructed, a numerical simulation is necessary for subsequent evaluation, with VISSIM serving as an appropriate tool for this purpose. To construct the simulation model, essential geometric details were derived from the Green Book (A Policy on Geometric Design of Highways and Streets) [61]. By taking these specified dimensions, the simulation model can accurately restore these designs. The critical details are as follows.

- The acceleration lane length is 300m, meeting the requirement specified in the Green Book.
- The auxiliary lane length is 450m, complying with the stipulations in the Green Book.
- The taper length is 180m, adhering to the Green Book's requirement for a 1:50 tapering rate.
- The speed limit lane length is 185m, satisfying the stipulated stopping sight distance at a speed limit of 100km/h as outlined in the Green Book.

IV. RESULT AND ANALYSIS

A. SIMULATION RESULT

Based on this description, simulation can be performed for the above five designs, including CTE, NTE, DATE, STE, and SATE. The following data were input into the VISSIM model according to the standard calibration procedure proposed in previous studies [42], [62].

- Geometric parameters for each design.
- The through and merging traffic volumes during the rush hour were 3187 and 1846, respectively, as listed in table 1, with the merging ratio of 36.7%.
- Trucks and Buses accounted for 7.6% of traffic, whereas the remaining 92.4% were cars.
- Speed of vehicles spread from 27.9 to 89.1km/h on the mainline and 24.8 to 57.2km/h on the ramp.

Table 2 shows the calculated results of the MAPE for the five designs, each of which is less than 5%. These calibration accuracies can be accepted in practical engineering applications, as indicated in previous studies [42], [43].

In addition, the authors entered more traffic situations into the VISSIM model to gain further verification. Figure 10 shows the fitting between the density and volume on the mainline from the simulation result. A visible peak occurred at the traffic volume of approximately 6000veh/h with a density of approximately 150veh/km, subsequently showing a decreasing trend that matches the actual. More than 99% goodness of fit of the quadratic polynomial also proves the significant compliance of the density and traffic volume with the Greenshields Model, which shows the rationality and accuracy of the VISSIM simulation.

The results of the simulation VISSIM with investigated data entered are listed in Table 3. Figure 11 shows the comparison of the performance of design schemes.

The results demonstrate the superior performance of all four enhanced designs compared with NTE under the investigated traffic conditions. DATE showed the most notable overall improvement, exhibiting enhancements of 7.2% in capacity, 3.1% in CO emissions, 45.3% in delays, and 49.0% in conflict. The other three enhanced designs also outperformed NTE in all aspects. Notably, SATE performed better than CTE in terms of delay, whereas CTE exhibited slightly lower levels of conflict. STE performs enhancements of 6.1% in capacity, 1.6% in CO emissions, 35.0% in delays, and 40.4% in conflicts.

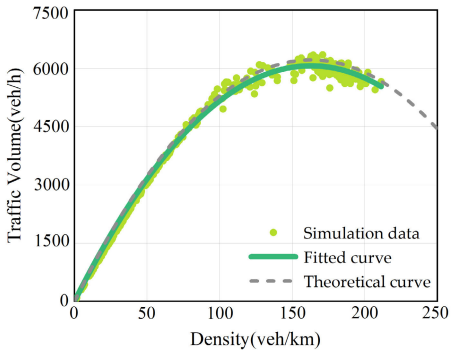

FIGURE 10. The correlation between density with traffic volume on the mainline in various traffic situations. Green dots denote simulation data, the green line denotes the fitted curve and the dotted line denotes the theoretical curve.

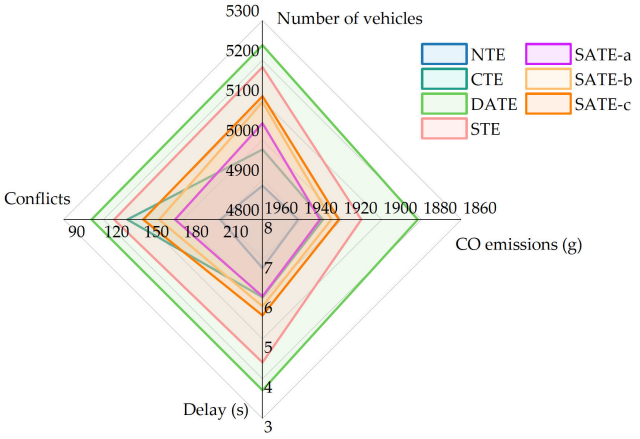

FIGURE 11. The comparison of the performance among the five designs in terms of CO emissions, delay, and conflicts.

B. SENSITIVITY ANALYSIS

With reference to the Capacity Manual, traffic volumes at 2460veh/h and 7200veh/h corresponding to the level of service A and E are taken as the boundary, then traffic volumes can be divided into seven groups according to a certain interval [62]. Considering that the merging ratio of the interchange should be less than 50%, 40%, and 10% are taken as the maximum and minimum bounds respectively. Thus, 28 situations with different traffic volumes and merging ratios are input into the VISSIM simulation. Table 4 presents the simulation schedule.

The three SATE schemes were initially compared to identify a superior design for subsequent analyses and evaluations. Since all three schemes offer the same additional capacity storage space, performance in terms of delay and conflict plays a crucial role in scheme comparison. The results are shown in Figure 12.

SATE-c works better under the vast majority of traffic, while SATE-b only shows slightly fewer conflicts under heavy traffic with a merging ratio of more than 30% and traffic volume of over 5620veh/h. Therefore, SATE-c was

TABLE 2. Results of the MAPE calculation for each design.

Flow	Average		Maximum		Minimum	
	Mainline	Ramp	Mainline	Ramp	Mainline	Ramp
Investigated capacity(veh/h)	3187	1846	3187	1846	3187	1846
Simulated capacity(veh/h)	3207	1871	3303	1935	3085	1800
Individual $MAPE_C(\%)$	0.63	1.35	3.67	4.76	-3.20	-2.55
$MAPE_C(\%)$	0.89		4.07		-2.94	
Investigated density(veh/km)	53.38	46.97	53.38	46.97	53.38	46.97
Simulated density(veh/km)	53.96	46.35	55.99	45.18	54.39	47.85
Individual $MAPE_D(\%)$	1.09	1.32	4.49	3.81	-1.89	-1.87
$MAPE_D(\%)$	1.19		4.20		-1.88	

TABLE 3. The operational performance of each design with investigation data.

Design Scheme	$Volume(veh/h)$	$COemissions(g)$	$Delay(s)$	$Conflicts$
NTE	4885	1942.011	6.78	198
CTE	4976	1929.557	6.05	128
DATE	5238	1881.889	3.71	101
STE	5183	1910.316	4.41	118
SATE-a	5042	1931.064	6.07	164
SATE-b	5095	1925.357	5.82	152
SATE-c	5110	1921.552	5.59	140

TABLE 4. Operational performance of each of the five designs using the investigation data.

Case	1	2	3	4	5	6	7
Traffic Volume(veh/h)	2460	3250	4040	4830	5620	6410	7200
Case	1	2	3	4			
Merging ratio(%)	10%	20%	30%	40%			

selected as the optimal design, serving as SATE in the final evaluation.

Subsequently, the performance of each design on different indicators was compared to NTE, it is clear that the four optimized schemes show different degrees of improvement in each aspect. Thus, an in-depth analysis of these various improvements is provided in this part.

Figure 13 shows the improvement of each optimized scheme compared to NTE in terms of capacity. Since higher capacity values imply better performance, the improvement ratio should be defined as Ratio = (Improved scheme - NTE)/NTE × 100%.

In Figure 13, it can be observed that the divide occurs around a volume of 5000veh/h, which corresponds to the beginning of a capacity bottleneck in NTE. As shown in Figure 10, traffic flows begin to collapse in NTE as flows exceed 6,000 veh/h, whereas the three-lane ramp demonstrated evident improvements in this regard. DATE exhibited the most substantial improvement, with a maximum ratio of 26.1%, which can be attributed to its enhanced storage capacity. STE and SATE follow suit, with improvement ratios related to the additional space they provide. CTE improved at a relatively low rate in most traffic situations. Consequently, it can be concluded that the three-lane ramp effectively alleviates capacity bottlenecks by offering additional capacity storage.

The opposite calculation to the improvement ratios of capacity was used for the other three indicators as they show better performance with lower values, it should be defined as Ratio = (NTE - Improved scheme)/NTE × 100%.

Figure 14(a) shows that CTE achieves the best improvement in the delay at low traffic volume and merging ratio, where the peak of 18.9% occurs at 3250veh/h volume and 10% merging ratio. Subsequently, the improvement faded rapidly as the volume increased. Similar trends are shown in Figure 14(d), where SATE shows a more significant peak in improvement rates under smoother traffic conditions. This phenomenon may be explained by the fact that SATE provides more space for smooth passage on the ramp and acceleration lane with less than a certain merging traffic volume. However, a more rapid decline in the improvement rate appears as traffic volumes increase, and congestion is even worse than CTE. This may be because vehicles on STAE change lanes more frequently, which will be limited by congested traffic, whereas this deficiency is not accentuated in a smooth traffic situation.

In contrast, DATE provides the best improvement rate with a minimum value of over 17.4%, closing to the peak of CTE, as shown in Figure 14(b). Moreover, the improvement ratio increases steadily with increasing traffic volume and merging ratio, which continues to the volume of 5620veh/h, with a peak of 45.6%. From Figure 14(c), it can be noticed that

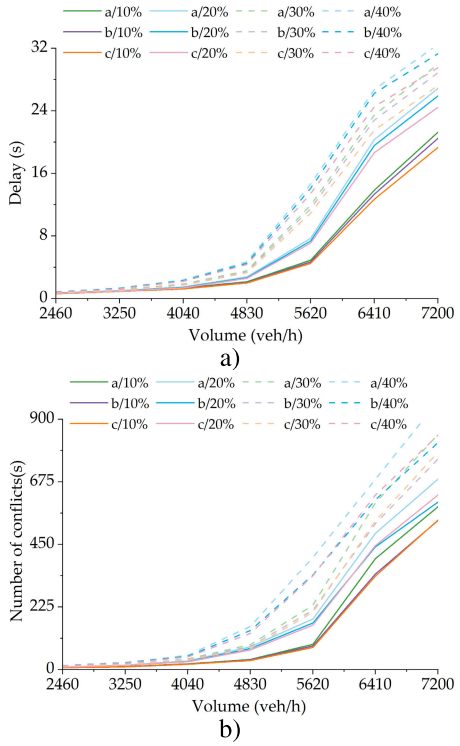

FIGURE 12. Comparison between the three SATE. (a)delay. (b)number of conflicts.

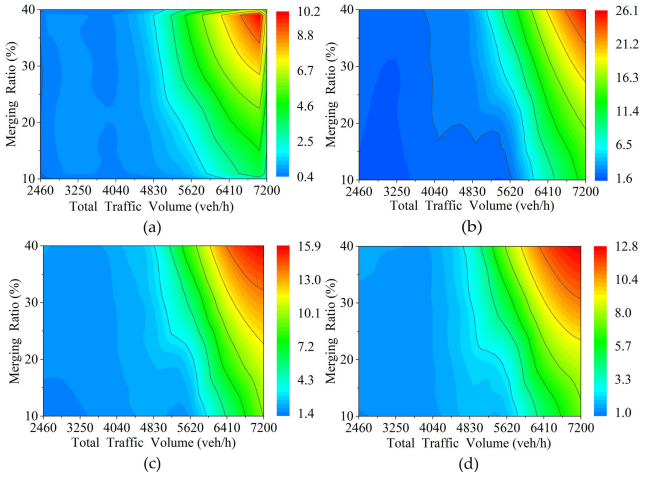

FIGURE 13. Improvement ratio of the scheme compared to NTE in terms of capacity(%). (a) CTE. (b)DATE. (c)STE. (d)SATE.

STE provides lower improvement rates compared to DATE, as well as it expires more quickly in heavy traffic situations. The three-lane ramp also shows limits to the improvement in delay, as the improvement ratios produce fading under overweight traffic, where the capacity bottleneck has been reached.

Figure 15 shows an improvement in CO emissions. At low traffic volumes, there is limited improvement because less congestion and delays are produced under low traffic pressure. In these cases, significant benefits are not prominently

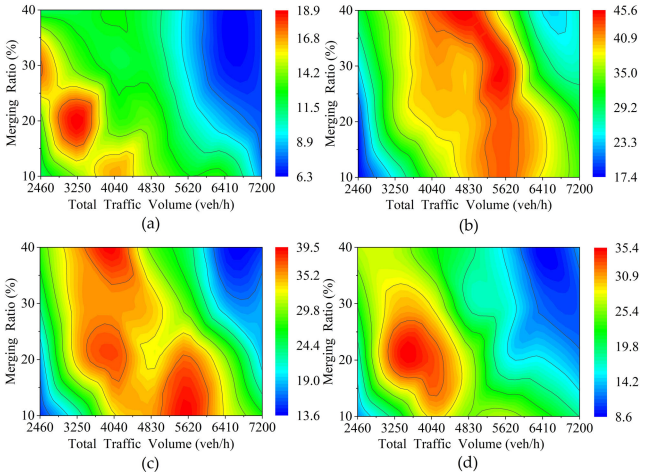

FIGURE 14. Improvement ratio of the scheme compared to NTE in terms of delay(%). (a) CTE. (b)DATE. (c)STE. (d)SATE.

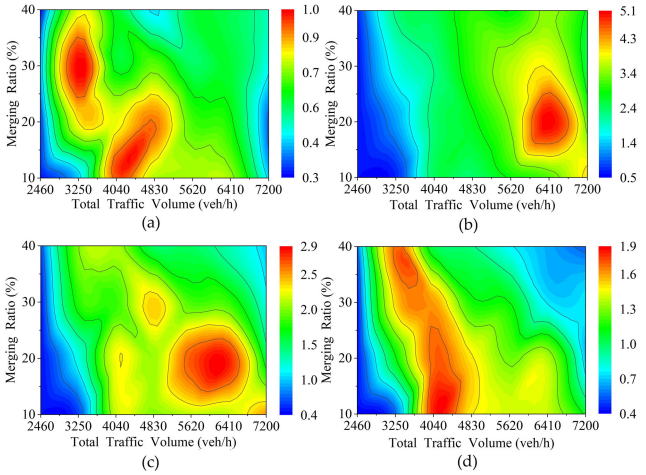

FIGURE 15. Improvement ratio of the scheme compared to NTE in terms of CO emission(%). (a) CTE. (b)DATE. (c)STE. (d)SATE.

visible due to the large emission base. Subsequently, as the traffic volume increased, the improvement in CO emissions also gradually increased. However, this improvement rapidly diminishes again with the arrival of capacity bottlenecks. Notably, the peak improvements in DATE and STE appear under heavier traffic conditions, attributable to improvements in capacity. Conversely, CTE and SATE reached their limits of carbon emission improvement earlier, highlighting their applicability in scenarios with smoother traffic flow.

As shown in Figure 16, all three three-lane ramp designs demonstrated the ability to improve conflict under heavy traffic, which may benefit from the increased capacity space. However, more frequent conflicts emerged in SATE during relatively smooth traffic conditions. These conflicts occurred primarily at the connections between the ramps and the auxiliary lanes, presumably because SATE required vehicles on all three ramps to merge into one auxiliary lane. Nevertheless, SATE again shows an improvement in conflicts

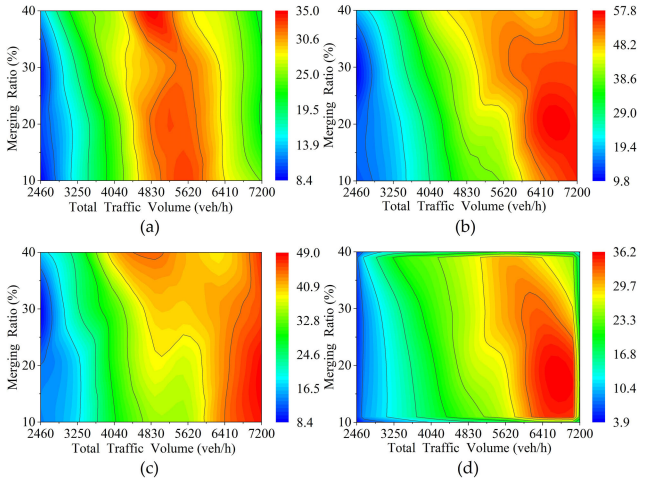

FIGURE 16. Improvement ratio of the scheme compared to NTE in terms of conflict(%). (a) CTE. (b)DATE. (c)STE. (d)SATE.

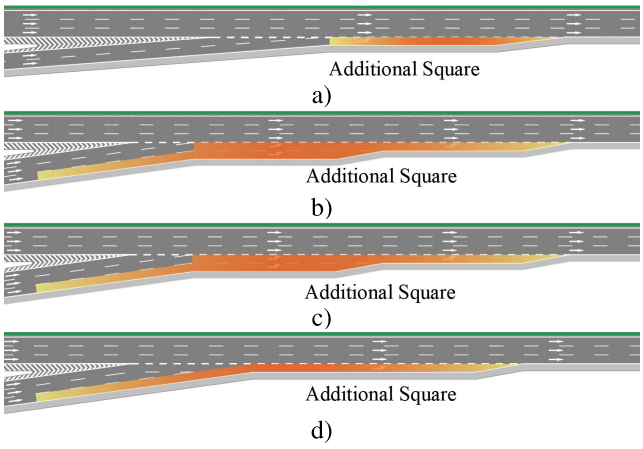

FIGURE 17. The additional square of each design in relation to the NTE. (a)CTE. (b)DATE. (c)STE. (d)SATE.

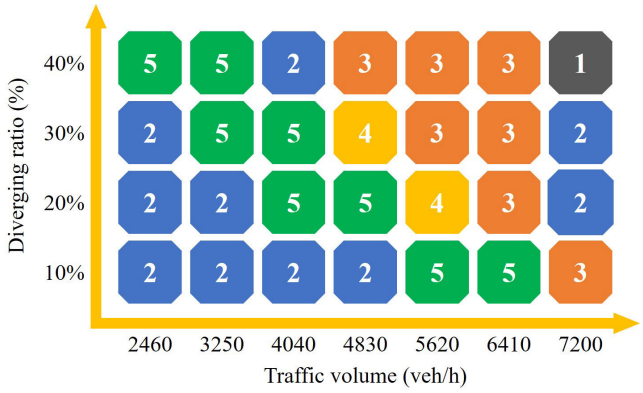

FIGURE 18. The optimal design for each situation, 1 to 5 denote NTE, CTE, DATE, STE, and SATE, respectively.

compared to CTE as traffic volumes increase. This may be attributed to the fact that the section is already congested and vehicle speeds are dropping dramatically. In this situation, more queuing space may be provided in SATE reducing conflicts.

C. EVALUATION RESULT

The sensitivity analysis provides a general judgment on the applicability of this design. Obviously, DATE performs substantially better than the other schemes in terms of traffic operations, with its potential being fully highlighted as traffic pressure increases. However, in situations of low traffic volumes and merger ratios, DATE fails to stand out as a significant advantage to offset its drawbacks of being more consumed in construction, and similar problems exist with other three-lane ramp designs. Therefore, the sensitivity analysis results can only provide a subjective reference for designers, while more decision-making details need to be obtained by objective and specific scoring using the CE.

Prior to the CE, it is essential to quantify the additional square of each design scheme, which is the fifth indicator selected. The additional square is defined as the increased area of the optimized solution behind the merging nose compared to NTE, as shown in Figure 17.

According to the CE procedure provided in Section II-E, weights assigned to each indicator for each traffic situation can be calculated, and each design scheme can be scored. Table 5 shows the results of the CRITIC calculated weights for the investigated traffic as an example, with 5033veh/h volume and 36.7% merging ratio. The results of the entropy method are also presented for comparison.

From the results, weights calculated from the entropy method exhibit a relatively average, which only concerns the single indicator value without their connection, creating an imbalance in the evaluation overly focused on traffic performance. The CRITIC method screens out the two main categories of traffic performance and construction cost through the interconnection of indicators, assigning more reasonable weights. It again highlights the advantages of the CE method provided in this paper.

Table 6 shows the final scoring results of the five designs for the investigated traffic situation through the TOPSIS with the CRITIC calculated weights, which suggests DATE is the optimal one.

The final score for each design under the 28 traffic situations was calculated based on the CE procedure, and the optimal design for each situation is listed in Figure 18.

V. DISCUSSION

As shown in Figure 18, CTE takes up several blocks at the bottom left, which corroborates with the information acquired in the sensitivity analysis. The performance of CTE does not significantly trail that of the three-lane ramp designs under smooth traffic conditions, as well as it requires less land space, thereby making it an appropriate choice under these conditions.

As the traffic volume and merging ratio increase, SATE emerges as the preferred optimal choice. SATE effectively

TABLE 5. Operational performance of the of five designs with investigation data.

Indexes		Capacity	Delay	CO emission	Conflicts	Additional square
CRITIC method	S_j	0.414	0.404	0.379	0.381	0.392
	R_j	2.222	2.220	2.185	2.252	6.829
	C_j	0.920	0.897	0.828	0.858	2.677
	Weights	14.905%	14.530%	13.407%	13.893%	43.365%
Entropy method	Weights	19.675%	22.076%	23.757%	14.928%	19.564%

TABLE 6. Operational performance of each design for investigated traffic situation.

Scheme	NTE	CTE	DATE	STE	SATE
D^+	0.7528	0.5409	0.6582	0.5294	0.4800
D^-	0.6582	0.5726	0.7528	0.5953	0.5424
Score	0.4665	0.5142	0.5335	0.5293	0.5305

utilizes an additional space in the merging areas, providing more capacity storage. Despite the fact that frequent lane changes due to vehicles entering the auxiliary lane from the ramp create a higher number of conflicts, SATE outperforms CTE in reducing delays. These improvements may be primarily derived from the deceleration lanes and ramps. However, it is essential to note that SATE's effectiveness is limited to relatively smooth traffic conditions, as it experiences gradual deterioration with increasing volume and merging ratio.

DATE occupies most of the blocks in the upper right triangle of the Figure. Despite the higher construction consumption and land occupation, the great potential of DATE under heavy traffic pressure remains a strong attraction for designers. In contrast, the STE is not considered to be a superior design in the vast majority of scenarios, being recommended in only rare cases. Overall, STE does not present a significant performance advantage over SATE, while it requires considerably more construction costs, thereby making it less attractive to designers.

Significantly, in the three right-most blocks, NTE and CTE reemerge as the best solutions. But in fact, CTE and NTE are not considered to support a smooth transition for traffic flow under these situations. Thus, this explains that all the improved designs fail in these cases because the mainline has been saturated, it is necessary to expand the entire mainline at this point.

For each case, the performance of capacity, delay, CO emissions, and conflicts in numerical value for the optimal design is compared with NTE, with the improvement ratio shown in Figure 19. For comparison, an additional square of the design is also listed. Similar reasons apply to CTE appearing at 4040veh/h volume and 40% merging ratio, in which SATE negligibly improves CTE or even shows more conflicts, yet the potential and advantages of DATE and STE have not been fully explored.

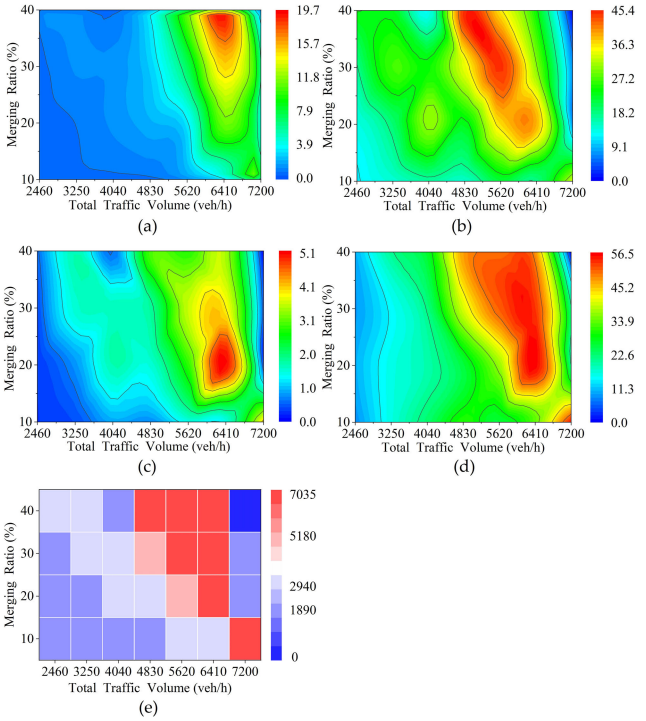

FIGURE 19. The improvement ratio of the optimal design in each case relative to NTE(%). (a) delay. (b) CO emissions. (c) number of conflicts. (d) additional square.

Figure 19 illustrates the significant improvement of the optimal design scheme for various traffic conditions compared to NTE, particularly under heavy traffic before the bottleneck is reached. The optimized design achieves the best benefits at 5000 to 6500veh/h volume, and the improvement ratio ranges around 15%, 40%, 4%, and 40% in capacity, delay, CO emissions, and conflicts respectively. In summary, as the traffic volume and merge ratio increase, it is necessary to optimize and expand NTE to achieve better traffic efficiency.

VI. CONCLUSION

Merging areas at interchanges are frequently regarded as bottlenecks that impede smooth traffic flows. Existing single or double-lane entrance ramps have become inadequate in accommodating increasing traffic. To address this issue, the authors propose a sustainable design method for three-lane entrance ramps to enhance operational efficiency in merging areas while minimizing resource consumption. Additionally,

the CE method is used to assess the applicability of these design schemes, thereby filling the gap in the design guidance for three-lane entrance ramps within the existing specifications.

Based on a certain interchange in Xi'an, this paper proposes several new three-lane entrance design strategies that are distinct from conventional practice. Then the VISSIM simulation model is developed and calibrated to evaluate the specific performance of each design in different traffic conditions. Four indicators including capacity, delay, CO emissions, and conflicts, were used to quantify the specific performance of each design in terms of efficiency, environmental protection, and safety. The additional square was also considered, measuring elements such as the cost and resource consumption of the construction. Finally, a CE method was developed based on the CRITIC method and TOPSIS, which assigns objective weights to indicators and scores for designs. Some significant conclusions drawn from this study are as follows

- Three-lane ramps provide more capacity storage and increase the capacity bottleneck in the merging area, which improves delays, CO emissions, and conflicts in traffic operation to varying degrees.
- DATE has the best comprehensive improvement, albeit not obvious under a low traffic volume and merging ratio. Its capacity is maximized under heavy traffic pressure, yet considering the high construction cost, it is mainly recommended to use at traffic volumes over 5000veh/h with a merging ratio of more than 20%.
- CTE and SATE perform better with volume below 4000veh/h or merging ratios below 10%. SATE provides more ramp capacity storage to improve delay and CO emissions on the ramp and acceleration lanes, but can also contribute to frequent lane changes to increase conflicts around the merging nose.
- Three-lane ramps also gradually fail once traffic volume exceeds 6400veh/h. At this point, the mainline capacity has reached saturation and congestion.
- The CE method provided in this paper demonstrates excellent superiority in the design evaluation of transportation. Because CRITIC considers the association between indicators more deeply compared with the traditional entropy method, which helps obtain a more rational weight assignment.

This paper shows the application of the sustainable design method and evaluation for the three-lane entrance ramp on Interchange *G*, because many expressways in urban areas face similar problems, this method can be supported for promotion. In the example in this paper, the consideration of the additional square is limited to the mainline, while in the specific engineering practice, the additional square and re-source consumption from the ramp expansion can be considered based on the actual design details, which would provide a more comprehensive and accurate result. The CE method based on the CRITIC method and TOPSIS proposed in this study provides designers with clear guidance and evidence for making decisions in scheme selection with convenient application. However, some additional issues still need to be researched before this method can be used in the future, such as whether it still provides an accurate assessment in more complex cases such as four-lane mainlines or adjacent continuous entrances.

REFERENCES

[1] R. Wang, J. Hu, and X. Zhang, "Analysis of the driver's behavior characteristics in low volume freeway interchange," *Math. Problems Eng.*, vol. 2016, pp. 1–9, Apr. 2016, doi: 10.1155/2016/2679516.

[2] Q. Wan, G. Peng, Z. Li, and F. H. T. Inomata, "Spatiotemporal trajectory characteristic analysis for traffic state transition prediction near expressway merge bottleneck," *Transp. Res. C, Emerg. Technol.*, vol. 117, Aug. 2020, Art. no. 102682, doi: 10.1016/j.trc.2020.102682.

[3] T. Fatema, K. Ismail, and Y. Hassan, "Validation of probabilistic model for design of freeway entrance speed change lanes," *Transp. Res. Rec., J. Transp. Res. Board*, vol. 2460, no. 1, pp. 97–106, Jan. 2014, doi: 10.3141/2460-11.

[4] A. T. McCartt, V. S. Northrup, and R. A. Retting, "Types and characteristics of ramp-related motor vehicle crashes on urban interstate roadways in northern Virginia," *J. Saf. Res.*, vol. 35, no. 1, pp. 107–114, Jan. 2004, doi: 10.1016/j.jsr.2003.09.019.

[5] K. Suzuki, K. Imada, and Y. Matsumura, "A study of collision risk estimation and users evaluation at merging section of urban expressway in Japan," *Transp. Res. Proc.*, vol. 15, pp. 783–793, Jan. 2016, doi: 10.1016/j.trpro.2016.06.065.

[6] J. Yuan, M. Abdel-Aty, Q. Cai, and J. Lee, "Investigating drivers' mandatory lane change behavior on the weaving section of freeway with managed lanes: A driving simulator study," *Transp. Res. F, Traffic Psychol. Behaviour*, vol. 62, pp. 11–32, Apr. 2019, doi: 10.1016/j.trf.2018.12.007.

[7] Y. Chung, H. Cho, and K. Choi, "Impacts of freeway accidents on CO_2 emissions: A case study for Orange County, California, US," *Transp. Res. D, Transp. Environ.*, vol. 24, pp. 120–126, Oct. 2013, doi: 10.1016/j.trd.2013.06.005.

[8] P. Li and S. Jones, "Vehicle restrictions and CO_2 emissions in Beijing—A simple projection using available data," *Transp. Res. D, Transp. Environ.*, vol. 41, pp. 467–476, Dec. 2015, doi: 10.1016/j.trd.2015.09.020.

[9] X. Chen, L. Jiang, Y. Xia, L. Wang, J. Ye, T. Hou, Y. Zhang, M. Li, Z. Li, Z. Song, J. Li, Y. Jiang, P. Li, X. Zhang, Y. Zhang, D. Rosenfeld, J. H. Seinfeld, and S. Yu, "Quantifying on-road vehicle emissions during traffic congestion using updated emission factors of light-duty gasoline vehicles and real-world traffic monitoring big data," *Sci. Total Environ.*, vol. 847, Nov. 2022, Art. no. 157581, doi: 10.1016/j.scitotenv.2022.157581.

[10] K. Zhang, S. Batterman, and F. Dion, "Vehicle emissions in congestion: Comparison of work zone, rush hour and free-flow conditions," *Atmos. Environ.*, vol. 45, no. 11, pp. 1929–1939, Apr. 2011, doi: 10.1016/j.atmosenv.2011.01.030.

[11] B. Lefèvre, "Long-term energy consumptions of urban transportation: A prospective simulation of 'transport-land uses' policies in Bangalore," *Energy Policy*, vol. 37, no. 3, pp. 940–953, Mar. 2009, doi: 10.1016/j.enpol.2008.10.036.

[12] F. I. Abam, E. B. Ekwe, O. E. Diemuodeke, M. I. Ofem, B. B. Okon, C. H. Kadurumba, A. Archibong-Eso, S. O. Effiom, J. G. Egbe, and W. E. Ukueje, "Environmental sustainability of the Nigeria transport sector through decomposition and decoupling analysis with future framework for sustainable transport pathways," *Energy Rep.*, vol. 7, pp. 3238–3248, Nov. 2021, doi: 10.1016/j.egyr.2021.05.044.

[13] L. C. Davis, "Mitigation of congestion at a traffic bottleneck with diversion and lane restrictions," *Phys. A, Stat. Mech. Appl.*, vol. 391, no. 4, pp. 1679–1691, Feb. 2012, doi: 10.1016/j.physa.2011.10.036.

[14] R. Salas, M. J. Perez-Villadoniga, J. Prieto-Rodriguez, and A. Russo, "Were traffic restrictions in Madrid effective at reducing NO_2 levels?" *Transp. Res. D, Transp. Environ.*, vol. 91, Feb. 2021, Art. no. 102689, doi: 10.1016/j.trd.2020.102689.

[15] X. Huang, Y. Zhang, W. Yang, Z. Huang, Y. Wang, Z. Zhang, Q. He, S. Lü, Z. Huang, X. Bi, and X. Wang, "Effect of traffic restriction on reducing ambient volatile organic compounds (VOCs): Observation-based evaluation during a traffic restriction drill in Guangzhou, China," *Atmos. Environ.*, vol. 161, pp. 61–70, Jul. 2017, doi: 10.1016/j.atmosenv.2017.04.035.

[16] D. Mohan, G. Tiwari, R. Goel, and P. Lahkar, "Evaluation of odd–even day traffic restriction experiments in Delhi, India," *Transp. Res. Rec., J. Transp. Res. Board*, vol. 2627, no. 1, pp. 9–16, Jan. 2017, doi: 10.3141/2627-02.

[17] K.-F. Lu, H.-W. Wang, X.-B. Li, Z.-R. Peng, H.-D. He, and Z.-P. Wang, "Assessing the effects of non-local traffic restriction policy on urban air quality," *Transp. Policy*, vol. 115, pp. 62–74, Jan. 2022, doi: 10.1016/j.tranpol.2021.11.005.

[18] S. Jia, Y. Li, and T. Fang, "Can driving-restriction policies alleviate traffic congestion? A case study in Beijing, China," *Clean Technol. Environ. Policy*, vol. 24, no. 9, pp. 2931–2946, Nov. 2022, doi: 10.1007/s10098-022-02377-z.

[19] Y.-Y. Chen, Y. Cheng, and G.-L. Chang, "Lane group-based traffic model for assessing on-ramp traffic impact," *J. Transp. Eng., A, Syst.*, vol. 147, no. 2, Feb. 2021, Art. no. 04020152, doi: 10.1061/JTEPBS.0000481.

[20] T. Bergh, K. Nordqvist, P. Strömgren, F. Davidsson, K. L. Bång, and A. Carlsson, "Capacity issues in Sweden—Applications and research," *Transp. Res. Proc.*, vol. 15, pp. 36–50, Jan. 2016, doi: 10.1016/j.trpro.2016.06.004.

[21] M. Alyamani and Y. Hassan, "Driver behavior on freeway entrance ramp terminals," *J. Transp. Eng., A, Syst.*, vol. 147, no. 12, Dec. 2021, Art. no. 04021090, doi: 10.1061/JTEPBS.0000606.

[22] X. Wan, P. J. Jin, F. Yang, and B. Ran, "Merging preparation behavior of drivers: How they choose and approach their merge positions at a congested weaving area," *J. Transp. Eng.*, vol. 142, no. 9, Sep. 2016, Art. no. 05016005, doi: 10.1061/(ASCE)TE.1943-5436.0000864.

[23] W. Hao, D. Rong, Z. Zhang, Y.-J. Byon, N. Lv, and Y. Chen, "Stability analysis and speed-coordinated control of mixed traffic flow in expressway merging area," *J. Transp. Eng., A, Syst.*, vol. 148, no. 11, Nov. 2022, Art. no. 04022098, doi: 10.1061/JTEPBS.0000755.

[24] A. Assadi, F. Meier, and L. D. Re, "Highway entrance merging assistant for minimal traffic disturbance," *IFAC-PapersOnLine*, vol. 53, no. 2, pp. 14267–14272, 2020, doi: 10.1016/j.ifacol.2020.12.1168.

[25] A. Spiliopoulou, M. Papageorgiou, J. C. Herrera, and J. C. Muñoz, "Real-time merging traffic control at congested freeway off-ramp areas," *Transp. Res. Rec., J. Transp. Res. Board*, vol. 2554, no. 1, pp. 101–110, Jan. 2016, doi: 10.3141/2554-11.

[26] R. X. Zhong, A. Sumalee, T. L. Pan, and W. H. K. Lam, "Optimal and robust strategies for freeway traffic management under demand and supply uncertainties: An overview and general theory," *Transportmetrica A, Transp. Sci.*, vol. 10, no. 10, pp. 849–877, Jan. 2014, doi: 10.1080/23249935.2013.871094.

[27] W. Shen and H. M. Zhang, "On the morning commute problem in a corridor network with multiple bottlenecks: Its system-optimal traffic flow patterns and the realizing tolling scheme," *Transp. Res. B, Methodol.*, vol. 43, no. 3, pp. 267–284, Mar. 2009, doi: 10.1016/j.trb.2008.07.004.

[28] M. Hunter, R. Machemehl, and A. Tsyganov, "Operational evaluation of freeway ramp design," in *Transp. Res. Rec.*, vol. 1751, pp. 90–100, Jan. 2001, doi: 10.3141/1751-11.

[29] P. Liu, H. Chen, J. J. Lu, and B. Cao, "How lane arrangements on freeway mainlines and ramps affect safety of freeways with closely spaced entrance and exit ramps," *J. Transp. Eng.*, vol. 136, no. 7, pp. 614–622, Jul. 2010, doi: 10.1061/(ASCE)TE.1943-5436.0000127.

[30] H. Sato, J. Xing, S. Tanaka, and K. Morikita, "Examining the effect of connecting auxiliary lanes on mitigation of expressway traffic congestion," *Int. J. Intell. Transp. Syst. Res.*, vol. 9, no. 2, pp. 55–63, May 2011, doi: 10.1007/s13177-011-0031-3.

[31] M. S. Shea, T. Q. Le, and R. J. Porter, "Combined crash frequency-crash severity evaluation of geometric design decisions: Entrance-exit ramp spacing and auxiliary lane presence," *Transp. Res. Rec., J. Transp. Res. Board*, vol. 2521, no. 1, pp. 54–63, Jan. 2015, doi: 10.3141/2521-06.

[32] Y. Qi, Y. Wang, X. S. Chen, R. L. Cheu, L. Yu, and H. Teng, "Methods of dropping auxiliary lanes at freeway weaving segments," *Transp. Planning Technol.*, vol. 41, no. 4, pp. 389–401, Mar. 2018, doi: 10.1080/03081060.2018.1453462.

[33] M. Asgharzadeh, P. S. Gubbala, A. Kondyli, and S. D. Schrock, "Effect of on-ramp demand and flow distribution on capacity at merge bottleneck locations," *Transp. Lett.*, vol. 12, no. 8, pp. 550–558, Sep. 2020, doi: 10.1080/19427867.2019.1665774.

[34] M. Asgharzadeh and A. Kondyli, "Effect of geometry and control on the probability of breakdown and capacity at freeway merges," *J. Transp. Eng., A, Syst.*, vol. 146, no. 7, Jul. 2020, Art. no. 04020055.

[35] X. Liu, C. Shao, S. Yang, R. Zhang, and B. Pan, "Study on the location of unconventional outside left-turn lane at signalized intersections based on an entropy method," *Frontiers Environ. Sci.*, vol. 10, Sep. 2022, Art. no. 970836, doi: 10.3389/fenvs.2022.970836.

[36] Q. Cai, M. Saad, M. Abdel-Aty, J. Yuan, and J. Lee, "Safety impact of weaving distance on freeway facilities with managed lanes using both microscopic traffic and driving simulations," *Transp. Res. Rec., J. Transp. Res. Board*, vol. 2672, no. 39, pp. 130–141, Dec. 2018, doi: 10.1177/0361198118780884.

[37] B. Ciuffo, V. Punzo, and M. Montanino, "Thirty years of Gipps' car-following model: Applications, developments, and new features," *Transp. Res. Rec., J. Transp. Res. Board*, vol. 2315, no. 1, pp. 89–99, Jan. 2012, doi: 10.3141/2315-10.

[38] G. Gomes, A. May, and R. Horowitz, "Congested freeway microsimulation model using VISSIM," in *Proc. 83rd Annu. Meeting Transp.-Res.-Board*, Jan. 2004, pp. 71–81, doi: 10.3141/1876-08.

[39] C. P. I. J. van Hinsbergen, W. J. Schakel, V. L. Knoop, J. W. C. van Lint, and S. P. Hoogendoorn, "A general framework for calibrating and comparing car-following models," *Transportmetrica A, Transp. Sci.*, vol. 11, no. 5, pp. 420–440, May 2015, doi: 10.1080/23249935.2015.1006157.

[40] J. Sun, Z. Li, and J. Sun, "Study on traffic characteristics for a typical expressway on-ramp bottleneck considering various merging behaviors," *Phys. A, Stat. Mech. Appl.*, vol. 440, pp. 57–67, Dec. 2015, doi: 10.1016/j.physa.2015.08.007.

[41] A. Kumar, B. Sah, A. R. Singh, Y. Deng, X. He, P. Kumar, and R. C. Bansal, "A review of multi criteria decision making (MCDM) towards sustainable renewable energy development," *Renew. Sustain. Energy Rev.*, vol. 69, pp. 596–609, Mar. 2017, doi: 10.1016/j.rser.2016.11.191.

[42] B. Pan, S. Luo, J. Ying, Y. Shao, S. Liu, X. Li, and J. Lei, "Evaluation and analysis of CFI schemes with different length of displaced left-turn lanes with entropy method," *Sustainability*, vol. 13, no. 12, p. 6917, Jun. 2021, doi: 10.3390/su13126917.

[43] Y. Shao, X. Han, H. Wu, and C. G. Claudel, "Evaluating signalization and channelization selections at intersections based on an entropy method," *Entropy*, vol. 21, no. 8, p. 808, Aug. 2019, doi: 10.3390/e21080808.

[44] D. Diakoulaki, G. Mavrotas, and L. Papayannakis, "Determining objective weights in multiple criteria problems: The critic method," *Comput. Oper. Res.*, vol. 22, no. 7, pp. 763–770, 1995, doi: 10.1016/0305-0548(94)00059-h.

[45] X. Zhang, Q. Zhang, and T. Sun, "Performance evaluation and obstacle factors analysis of urban public transport priority," *Transp. Planning Technol.*, vol. 42, no. 7, pp. 696–713, Oct. 2019, doi: 10.1080/03081060.2019.1650433.

[46] Z. Tian and S. Zhang, "Application of multi-attribute group decision-making methods in urban road traffic safety evaluation with interval-valued intuitionistic fuzzy information," *J. Intell. Fuzzy Syst.*, vol. 40, no. 3, pp. 5337–5346, Mar. 2021, doi: 10.3233/jifs-202142.

[47] J. Zhang, Y. Tu, J. Liu, L. Liu, and Z. Li, "Regional public transportation safety risk grading assessment under time dimension: A case study of Chinese mainland," *Transp. Policy*, vol. 126, pp. 343–354, Sep. 2022, doi: 10.1016/j.tranpol.2022.08.003.

[48] M. Kumari and M. S. Kulkarni, "A unified index for proactive shop floor control," *Int. J. Adv. Manuf. Technol.*, vol. 100, nos. 9–12, pp. 2435–2454, Feb. 2019, doi: 10.1007/s00170-018-2683-5.

[49] M. K. Ghorabaee, M. Amiri, E. K. Zavadskas, and J. Antucheviciene, "A new hybrid fuzzy MCDM approach for evaluation of construction equipment with sustainability considerations," *Arch. Civil Mech. Eng.*, vol. 18, no. 1, pp. 32–49, Jan. 2018, doi: 10.1016/j.acme.2017.04.011.

[50] Q.-H. Zhao, X. Zhou, R.-F. Xie, and Z.-C. Li, "Comparison of three weighing methods for evaluation of the HPLC fingerprints of cortex fraxini," *J. Liquid Chromatography Rel. Technol.*, vol. 34, no. 17, pp. 2008–2019, Oct. 2011, doi: 10.1080/10826076.2011.582912.

[51] J. R. San Cristóbal, "Multi-criteria decision-making in the selection of a renewable energy project in Spain: The Vikor method," *Renew. Energy*, vol. 36, no. 2, pp. 498–502, Feb. 2011, doi: 10.1016/j.renene.2010.07.031.

[52] A. Ruiz-Padillo, D. P. Ruiz, A. J. Torija, and Á. Ramos-Ridao, "Selection of suitable alternatives to reduce the environmental impact of road traffic noise using a fuzzy multi-criteria decision model," *Environ. Impact Assessment Rev.*, vol. 61, pp. 8–18, Nov. 2016, doi: 10.1016/j.eiar.2016.06.003.

[53] Z. Stirbanović, D. Stanujkić, I. Miljanović, and D. Milanović, "Application of MCDM methods for flotation machine selection," *Minerals Eng.*, vol. 137, pp. 140–146, Jun. 2019, doi: 10.1016/j.mineng.2019.04.014.

[54] Z. Stirbanović, V. Gardić, D. Stanujkić, R. Marković, J. Sokolović, and Z. Stevanović, "Comparative MCDM analysis for AMD treatment method selection," *Water Resour. Manag.*, vol. 35, no. 11, pp. 3737–3753, Sep. 2021, doi: 10.1007/s11269-021-02914-3.

[55] Y. Wang, P. Liu, and Y. Yao, "BMW-TOPSIS: A generalized TOPSIS model based on three-way decision," *Inf. Sci.*, vol. 607, pp. 799–818, Aug. 2022, doi: 10.1016/j.ins.2022.06.018.

[56] Y. Shao, H. Yu, H. Wu, X. Han, X. Zhou, C. G. Claudel, H. Zhang, and C. Yang, "Evaluation of an exclusive spur dike U-turn design with radar-collected data and simulation," *J. Visualized Exp.*, no. 156, Feb. 2020, doi: 10.3791/60675.
[57] J. Zhao, P. Li, and X. Zhou, "Capacity estimation model for signalized intersections under the impact of access point," *PLoS ONE*, vol. 11, no. 1, Jan. 2016, Art. no. e0145989, doi: 10.1371/journal.pone.0145989.
[58] D. Henclewood, W. Suh, M. O. Rodgers, R. Fujimoto, and M. P. Hunter, "A calibration procedure for increasing the accuracy of microscopic traffic simulation models," *Simulation*, vol. 93, no. 1, pp. 35–47, Jan. 2017, doi: 10.1177/0037549716673723.
[59] J. Wang, Y. Mao, J. Li, Z. Xiong, and W.-X. Wang, "Predictability of road traffic and congestion in urban areas," *PLoS ONE*, vol. 10, no. 4, Apr. 2015, Art. no. e0121825, doi: 10.1371/journal.pone.0121825.
[60] S. Li, Q. Xiang, Y. Ma, X. Gu, and H. Li, "Crash risk prediction modeling based on the traffic conflict technique and a microscopic simulation for freeway interchange merging areas," *Int. J. Environ. Res. Public Health*, vol. 13, no. 11, p. 1157, Nov. 2016, doi: 10.3390/ijerph13111157.
[61] *A Policy on Geometric Design of Highways and Streets*, 7th ed. Washington, DC, USA: American Association of State Highway and Transportation Officials, 2018.
[62] Y. Xiang, Z. Li, W. Wang, J. Chen, H. Wang, and Y. Li, "Evaluating the operational features of an unconventional dual-bay U-turn design for intersections," *PLoS ONE*, vol. 11, no. 7, Jul. 2016, Art. no. e0158914, doi: 10.1371/journal.pone.0158914.

YUTONG LIU was born in Anhui, China, in 1999. He received the B.S. degree in civil engineering infrastructure from Chang'an University, Xi'an, China, in 2020, where he is currently pursuing the Ph.D. degree.

His research interests include road and interchange geometry design, traffic congestion and safety, traffic data analysis, and sustainable transportation.

BINGHONG PAN was born in Wuhan, Hubei, China, in 1974. He received the B.S., M.S., and Ph.D. degrees in transportation engineering from Chang'an University, Xi'an, Shaanxi, China, in 1996, 1999, and 2008, respectively.

He is currently an Associate Professor with the Highway Academy, Chang'an University. His research interests include highway engineering, interchange design, and traffic safety.

Dr. Pan was a recipient of the 2013 Science and Technology Award from the China Highway and Transportation Association.

RUIHUA SONG was born in Hebei, China, in 2000. She received the B.S. degree in traffic and transportation engineering from Shijiazhuang Tiedao University, China, in 2022. She is currently pursuing the master's degree with Chang'an University.

Her research interests include road and interchange design, sustainable transportation, highway engineering, traffic safety, and road engineering.

LIN ZONG was born in Henan, China, in 1997. He received the B.S. and M.S. degrees in transportation engineering from Chang'an University, Xi'an, Shaanxi, China, in 2019 and 2022, respectively.

His research interests include road engineering and traffic safety.